Cell Transplantation, Vol. 26, pp. 513–527, 2017
Printed in the USA.

0963-6897/17 $90.00 + .00
DOI: https://doi.org/10.3727/096368916X694265
E-ISSN 1555-3892
www.cognizantcommunication.com

Imbalanced Production of Reactive Oxygen Species and Mitochondrial Antioxidant SOD2 in Fabry Disease-Specific Human Induced Pluripotent Stem Cell-Differentiated Vascular Endothelial Cells

Wei-Lien Tseng,*†[1] Shih-Jie Chou,*[1] Huai-Chih Chiang,†‡ Mong-Lien Wang,§ Chian-Shiu Chien,†§ Kuan-Hsuan Chen,‡¶ Hsin-Bang Leu,§#** Chien-Ying Wang,§†† Yuh-Lih Chang,*¶ Yung-Yang Liu,‡††† Yuh-Jyh Jong,‡‡§§¶¶ Shinn-Zong Lin,## Shih-Hwa Chiou,*†‡§ Shing-Jong Lin,†‡§** and Wen-Chung Yu§**

*Institute of Pharmacology, National Yang-Ming University, Taipei, Taiwan
†Department of Medical Research, Taipei Veterans General Hospital, Taipei, Taiwan
‡Institute of Clinical Medicine, National Yang-Ming University, Taipei, Taiwan
§School of Medicine, National Yang-Ming University, Taipei, Taiwan
¶Department of Pharmacology, Taipei Veterans General Hospital, Taipei, Taiwan
#Heath Care and Management Center, Taipei Veterans General Hospital, Taipei, Taiwan
**Division of Cardiology, Department of Medicine, Taipei Veterans General Hospital, Taipei, Taiwan
††Department of Emergency Medicine, Taipei Veterans General Hospital, Taipei, Taiwan
‡‡Department of Biological Science and Technology, National Chiao Tung University, Hsinchu, Taiwan
§§Graduate Institute of Clinical Medicine, College of Medicine, Kaohsiung Medical University, Kaohsiung, Taiwan
¶¶Departments of Pediatrics and Laboratory Medicine, Kaohsiung Medical University Hospital, Kaohsiung Medical University, Kaohsiung, Taiwan
##Buddhist Tzu Chi General Hospital, Hualien, Taiwan

Fabry disease (FD) is an X-linked inherited lysosomal storage disease caused by α-galactosidase A (GLA) deficiency. Progressive intracellular accumulation of globotriaosylceramide (Gb3) is considered to be pathogenically responsible for the phenotype variability of FD that causes cardiovascular dysfunction; however, molecular mechanisms underlying the impairment of FD-associated cardiovascular tissues remain unclear. In this study, we reprogrammed human induced pluripotent stem cells (hiPSCs) from peripheral blood cells of patients with FD (FD-iPSCs); subsequently differentiated them into vascular endothelial-like cells (FD-ECs) expressing CD31, VE-cadherin, and vWF; and investigated their ability to form vascular tube-like structures. FD-ECs recapitulated the FD pathophysiological phenotype exhibiting intracellular Gb3 accumulation under a transmission electron microscope. Moreover, compared with healthy control iPSC-derived endothelial cells (NC-ECs), reactive oxygen species (ROS) production considerably increased in FD-ECs. Microarray analysis was performed to explore the possible mechanism underlying Gb3 accumulation-induced ROS production in FD-ECs. Our results revealed that superoxide dismutase 2 (SOD2), a mitochondrial antioxidant, was significantly downregulated in FD-ECs. Compared with NC-ECs, AMPK activity was significantly enhanced in FD-ECs. Furthermore, to investigate the role of Gb3 in these effects, human umbilical vein endothelial cells (HUVECs) were treated with Gb3. After Gb3 treatment, we observed that SOD2 expression was suppressed and AMPK activity was enhanced in a dose-dependent manner. Collectively, our results indicate that excess accumulation of Gb3 suppressed SOD2 expression, increased ROS production, enhanced AMPK activation, and finally caused vascular endothelial dysfunction. Our findings suggest that dysregulated mitochondrial ROS may be a potential target for treating FD.

Key words: Fabry disease (FD); Vascular endothelial dysfunction; Superoxide dismutase 2 (SOD2); Gb3 accumulation; Induced pluripotent stem cells (iPSCs)

Received June 30, 2016; final acceptance December 21, 2016. Online prepub date: December 6, 2016.
[1]These authors provided equal contribution to this work.
Address correspondence to Wen-Chung Yu, Division of Cardiology, Department of Medicine, Taipei Veterans General Hospital, No. 201, Sec. 2 Shih-Pai Road, Taipei 11217, Taiwan. Tel: 886-2-28757394; Fax: 886-2-28757435; E-mail: wcyu@vghtpe.gov.tw

INTRODUCTION

Fabry disease (FD) is a glycosphingolipid lysosomal storage disorder resulting from the mutational deficiency of α-galactosidase A (GLA) and characterized by progressive accumulation of cellular globotriaosylceramide (Gb3), particularly in vascular endothelial and smooth muscle cells[1,2]. To date, 672 GLA mutations have been reported[3], and the IVS4+919G>A mutation is the most common type of GLA mutation detected in Taiwanese patients with FD[4–6]. Clinical studies have reported that FD-associated dysfunction of vascular endothelial cells (VECs) plays a critical role in the pathogenesis of atherosclerosis in the small arteries and arterioles[7] and medium-sized radial artery[8]. In addition, functional disturbance of endothelium-dependent vasodilatory pathways has been reported in patients with FD[9].

Accumulation of Gb3 in human endothelial cells (ECs) significantly affects endothelial functions[10]. Furthermore, administration of Gb3 to ECs induced the degradation of the membrane Ca^{2+}-activated K^+ channel ($K_{Ca}3.1$) that causes dysregulation of endothelium-dependent relaxation[11]. Moreover, massive accumulation of intracellular Gb3 dysregulates the production of reactive oxygen species (ROS) and expression of cell adhesion molecules in ECs[12,13]. Overproduction of intracellular ROS has been implicated in the pathogenesis of cardiovascular diseases through the subsequent stimulation of proinflammatory cascade events[14,15]. Furthermore, inflammatory cells produce abundant ROS and secrete inflammatory cytokines and chemokines that further contribute to endothelial dysfunction[16].

Antioxidant enzymes such as superoxide dismutase (SOD), catalase, and glutathione peroxidase (GPX) are critical ROS scavengers in the cardiovascular system and protect the endothelium from endogenous and exogenous oxidative stress, inflammatory overreaction, and physiological impairment[17]. Among the antioxidant enzymes, SOD2 plays a critical role in protecting the cardiovascular system[18]. SOD2, also termed as manganese SOD, is a mitochondrial matrix protein required for protecting cells from ROS[19]. Deficiency in SOD2 expression results in vascular endothelial dysfunction[20–23], suggesting that SOD2 has a vital role in maintaining cellular and mitochondrial redox balance in VECs. However, whether excess accumulation of intracellular Gb3 affects the dysregulation of ROS production and imbalance of SOD2-dependent mitochondrial antioxidants in FD and FD-associated vascular endothelial dysfunction remains unclear.

Human induced pluripotent stem cells (hiPSCs) are a powerful tool with abilities of unlimited expansion and lineage-specific differentiation and can be used as a potential model of inherent diseases to study their underlying pathogenic mechanisms[24]. Although hiPSCs derived from a patient with FD have been recently applied in the study of FD-associated cardiomyopathy[25], to the best of our knowledge, a hiPSC-derived vascular endothelial model has not yet been established for studying FD-associated endothelial dysfunction. In this study, hiPSCs derived from a patient carrying the GLA IVS4+919G>A mutation were differentiated into endothelial-like cells expressing the vascular endothelial markers CD31 and von Willebrand factor (vWF). In addition, we investigated the molecular basis of increased ROS production induced by GLA deficiency in the ECs of patients with FD.

MATERIALS AND METHODS

Generation and Culture of hiPSCs

We generated hiPSCs from peripheral blood mononuclear cells (PBMCs) according to a previous study[26]. Peripheral blood samples from patients with FD receiving enzyme replacement therapy (ERT) were collected by qualified clinicians. All procedures, including those for blood tests and biopsy samples, were approved by the institutional review board of Taipei Veterans General Hospital (TVGH-IRB), and signed patient consent forms were obtained. PBMCs were isolated from peripheral blood using Histopaque-1077 (Sigma-Aldrich, St. Louis, MO, USA) through centrifugation at 400×*g* for 30 min. The buffy coat was collected, washed with phosphate-buffered saline (PBS), and maintained in X-VIVO 10 (Lonza, Basel, Switzerland) for 2 days. Furthermore, PBMCs (2×10^6) were reprogrammed by transfecting a mixture of plasmids containing PCXLE-hOCT3/4-shp53 (0.83 μg), PCXLE-hSK (0.83 μg), pCXLE-hUL (0.83 μg), and pCXWB-EBNA1 (0.5 μg) using the Amaxa™ Human T Cell Nucleofector™ kit and Amaxa Nucleofector II Program V-024 (Lonza). PBMCs were then cocultured with inactivated mouse embryonic fibroblasts as feeder cells and activated using interleukin-2 (IL-2) (175 U/ml) (PeproTech, Rocky Hill, NJ, USA) and Dynabead T-Activator CD3/CD28 (3.75 μl/ml; Thermo Fisher Scientific, Grand Island, NY, USA) in human embryonic stem cell medium containing Dulbecco's modified Eagle's medium (DMEM)/F12 (Thermo Fisher Scientific, Waltham, MA, USA) supplemented with 20% KnockOut Serum Replacement (KSR; Thermo Fisher Scientific), 0.1 mM nonessential amino acids (Thermo Fisher Scientific), 1 mM L-glutamine (Thermo Fisher Scientific), 0.1 mM β-mercaptoethanol (Sigma-Aldrich), 10 ng/ml recombinant human basic fibroblast growth factor (hbFGF) (PeproTech), and antibiotics (Thermo Fisher Scientific). The medium was replaced with fresh medium every 2 days. Alkaline phosphatase (ALP)-positive hiPSC colonies were selected from day 21 to day 28 after nucleofection; undifferentiated hiPSCs were transferred to a Geltrax (Thermo Fisher Scientific)-coated culture dish and cultured in mTeSR1 medium (StemCell Technologies, Vancouver, Canada).

Differentiation of ECs

We differentiated hiPSCs to ECs according to the established monolayer EC differentiation protocol[27] with a minor modification. Briefly, hiPSC clumps were seeded into a six-well plate coated with Geltrax and incubated with STEMdiff™ APEL™ endoderm differentiation medium (StemCell Technologies) containing activin A (25 ng/ml; Cayman, Ann Arbor, MI, USA), BMP4 (30 ng/ml; Cayman), CHIR (1.5 mM; Cayman), and vascular endothelial growth factor (VEGF; 50 ng/ml; R&D Systems, Minneapolis, MN, USA). After 3 days, the medium was exchanged to STEMdiff™ APEL™ containing VEGF (50 ng/ml) and SB431542 (10 nM; TOCRIS, Bristol, UK) and continuously changed at days 10 and 13. ECs were isolated at day 14 using CD31-conjugated magnet beads (StemCell Technologies). Isolated ECs were further cultured in endothelial cell growth medium-2 (EGM-2) (Lonza) complemented with 5 % fetal bovine serum (FBS).

Tube Formation Assay

Tube formation assay was performed using μ-slide angiogenesis (Ibidi, Martinsried, Germany) following the manufacturer's instructions. Briefly, 1×10^4 cells were plated onto Matrigel (BD Biosciences, San Jose, CA, USA)-coated μ-slide with EGM-2 medium (Lonza). After 6 h, cells were stained with calcein AM (Sigma-Aldrich). The endothelial network was observed through fluorescence microscopy.

Immunofluorescence

Immunofluorescence staining was performed as described previously with some modifications[26]. Cells were fixed with 1% paraformaldehyde (PFA) (Sigma-Aldrich) solution at room temperature for 15 min and permeabilized with 0.1% Triton X-100 (Merck, Darmstadt, Germany) for 10 min. After several washes with 1× PBS, fixed cells were blocked using 3% bovine serum albumin (BSA; Bovogen Biologicals, VIC, Australia) and 5% FBS and consequently incubated with indicated monoclonal antibodies (1:100) at 4°C overnight. Cells were washed thrice with PBS and incubated with the cyanine 3 (Cy3)- or Cy5-conjugated donkey anti-mouse secondary antibody (Thermo Fisher Scientific) at room temperature for 1 h. Finally, cells were mounted and observed using a fluorescent or FV10i confocal microscope (Olympus, Center Valley, PA, USA).

ALP Staining

ALP staining was performed using the blue alkaline phosphatase substrate kit (Vector Laboratories, Burlingame, CA, USA) following the manufacturer's instructions. Briefly, cells were washed twice with PBS and fixed with 80% alcohol for at least 2 h at 4°C. Then alcohol and infiltrated cells were aspirated using double-distilled water for 2 min. After infiltration, Tris-HCl (100 mM, pH 8.2–8.5) was added for 5 min followed by replacement with the working solution of ALP substrate for 1 h. Colonies that were stained purple indicated positive ALP activity.

Transmission Electron Microscopy

The indicated cells were fixed in 4% PFA, 2% glutaraldehyde (both from Electron Microscopy Sciences, Hatfield, PA, USA), and 0.1 M phosphate buffer at 4°C overnight and then embedded in epoxy resin and sectioned. Ultrathin sections were counterstained with 2.5% uranyl acetate (Electron Microscopy Sciences) and 0.4% lead citrate (Sigma-Aldrich) and then observed using the JEM-2000EXII (JEOL, Tokyo, Japan) electron microscope.

Microarray and Quantitative Real-Time PCR

Total RNA was isolated using TRIzol (Thermo Fisher Scientific). The samples were processed and hybridized to Affymetrix GeneChip Human Genome U133 2.0 Arrays according to the Affymetrix GeneChip Expression Analysis Technical Manual (Affymetrix, Santa Clara, CA, USA).

For quantitative real-time polymerase chain reaction (qRT-PCR), 0.5 μg of total RNA was reverse transcribed with SuperScript III (Thermo Fisher Scientific) into cDNA as the template for the following RT-PCR. The RT-PCR program was performed on an ABI 7900 (Thermo Fisher Scientific) with indicated primer sets (Table 1) using the following conditions: initial denaturation at 95°C for

Table 1. Primers for Quantitative PCR

Gene ID	Primer Sequence	T_m	Product Size (bp)
SOD1	F: CCACACCTTCACTGGTCCAT	53.7	109
	R: CTAGCGAGTTATGGCGACG	53.1	
SOD2	F: TAGGGCTGAGGTTTGTCCAG	53.7	125
	R: GGAGAAGTACCAGGAGGCGT	55.8	
SOD3	F: CGAGTCAGAGTTGGGCTCC	55.3	130
	R: TCTCTTGGAGGAGCTGGAAA	51.7	
GAPDH	F: AGAAGGCTGGGGCTCATTTG	53.7	258
	R: AGGGGCCATCCACAGTCTTC	57.8	

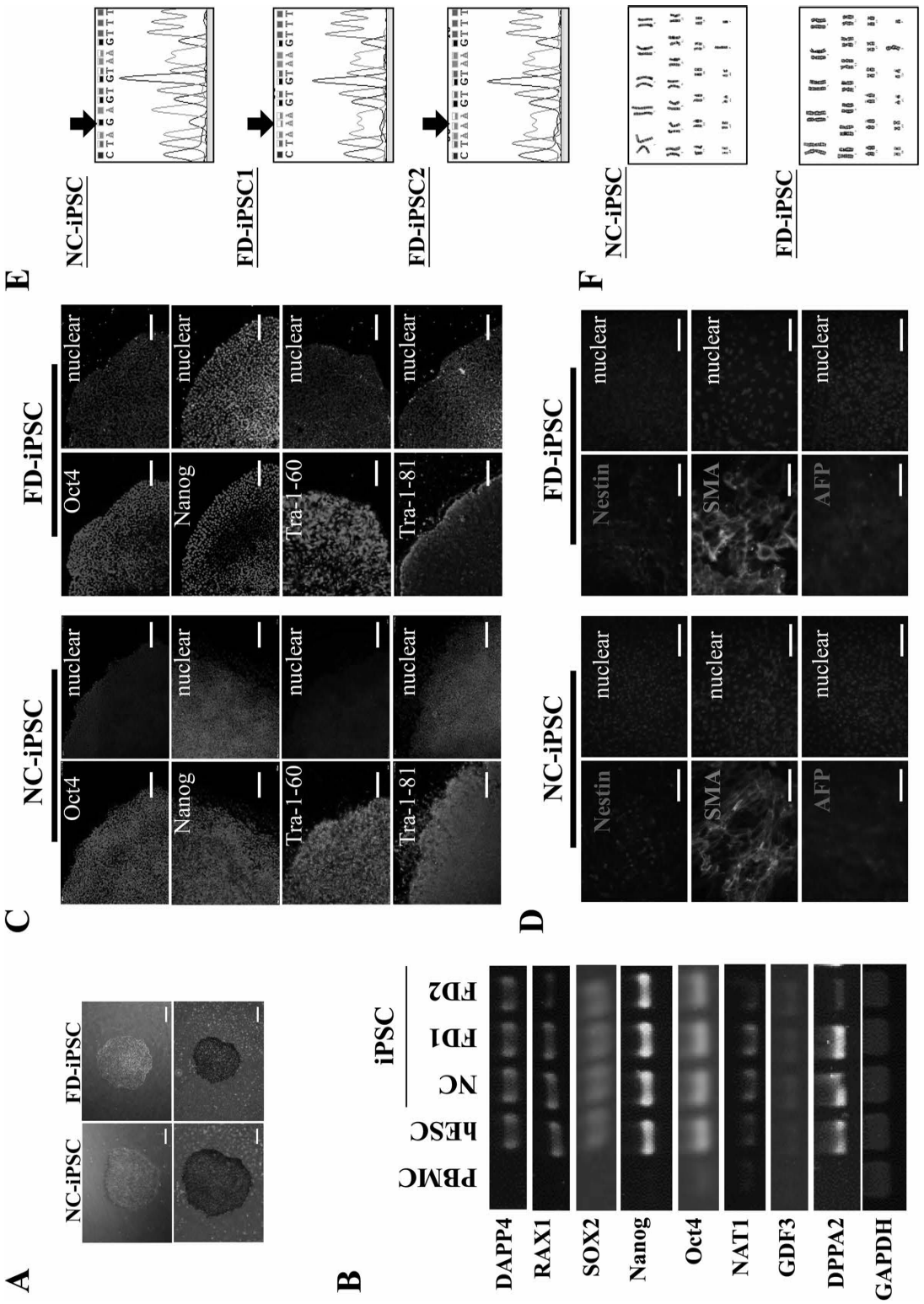

10 min and repeated 40 cycles of 95°C for 15 s and 60°C for 1 min.

Immunoblotting

Total proteins were separated through gradient sodium dodecyl sulfate polyacrylamide gel electrophoresis (SDS-PAGE) and transferred onto a polyvinylidene difluoride (PVDF) membrane. After blocking with 5% skim milk at room temperature for 1 h, the membrane was hybridized with indicated primary antibodies in Tris-buffered saline Tween 20 (TBST) buffer solution at 4°C overnight, followed by incubation with horseradish peroxidase-conjugated secondary antibodies at RT for 1 h. The immunoblot was developed using an enhanced chemiluminescence system (EMD Millipore, Darmstadt, Germany) and detected using an X-ray film (Fujifilm, Tokyo, Japan).

Cellular ROS and Mitochondrial ROS Assay

The cellular and mitochondrial levels of ROS were determined using 2′,7′-dichlorofluorescin diacetate (DCFDA; Sigma-Aldrich) and MitoSOX Red (Thermo Fisher Scientific), respectively. The cells were washed with PBS twice and incubated with 100 μM DCFDA or MitoSOX red in a loading medium in a CO_2 incubator at 37°C for 30 min. The cells were then washed with PBS. Fluorescence was measured through flow cytometry.

Conjugation of Gb3 With BSA and Loading on Human Umbilical Vein ECs

Human umbilical vein ECs (HUVECs) were cultured in EGM-2 medium. We administered Gb3 (Matreya, Pleasant Gap, PA, USA) to ECs following a previous description with some modifications[10]. Briefly, Gb3 was dissolved in chloroform (Merck)/methanol (2:1 by volume) in a glass tube and left for air drying, followed by resuspension in dimethyl sulfoxide (DMSO) (Sigma-Aldrich). Gb3–DMSO was heated at 90°C for 10 min with occasional vortexing. Subsequently, the Gb3 solution was mixed with PBS containing fatty acid-free BSA to achieve a 1:1 molar ratio of Gb3/albumin. The Gb3–albumin complex was formed through sonication in a bath sonicator for 10 min. Finally, the Gb3–albumin complex was diluted into EGM-2 medium containing 0.5% FBS. HUVECs were incubated with the medium containing the indicated concentration of the Gb3–albumin complex or recombinant human α-galactosidase A (rhα-GLA; Genzyme Corporation, Cambridge, MA, USA) for 48 h.

Statistical Analysis

Data are presented as mean±standard error of the mean (SEM). Statistical analyses were performed using GraphPad Prism, Version 5.00 (GraphPad Software, La Jolla, CA, USA). Statistical significance was assessed using unpaired Student's *t*-test or one-way analysis of variance (ANOVA) followed by Bonferroni multiple comparisons test. A value of $p<0.05$ was considered statistically significant.

RESULTS

Establishment of hiPSCs and hiPSC-Derived VECs From PBMCs of a Patient With FD

PBMCs isolated from a patient with FD carrying the GLA IVS4+919G>A mutation were reprogrammed to induced pluripotent stem cells (iPSCs; FD-iPSCs) through transfection of nonviral plasmids using the electroporation method[26]. The characteristics of the generated FD-iPSCs were examined. As presented in Figure 1A, both FD-iPSCs and healthy control-derived iPSCs (NC-iPSC) exhibited EC-like morphology and positive staining for ALP. The mRNA expression levels of stem cell genes (*DAPP4*, *RAX1*, *SOX2*, *NANOG*, *OCT4*, *NAT1*, *GDF3*, and *DAPP2*) in FD-iPSCs and NC-iPSCs were similar to those in human embryonic stem cells (hESCs) (Fig. 1B). In addition, the protein expression of human pluripotent stem cell markers [octamer-binding transcription factor 4 (OCT4), NANOG, TRA-1-60, and TRA-1-81] in both FD-iPSCs and NC-iPSCs was determined using immunofluorescence staining (Fig. 1C). Under in vitro three-germ

FACING PAGE

Figure 1. Generation and characterization of Fabry disease-specific induced pluripotent stem cells (FD-iPSCs) carrying the α-galactosidase A (*GLA)* IVS4+919G>A mutation. (A) Morphology and alkaline phosphatase activity of FD-iPSCs. Scale bars: 100 μm. (B) Reverse transcription polymerase chain reaction (RT-PCR) analysis indicated the expression pattern of embryonic stem cell-like genes in FD-iPSC sublines. Human embryonic stem cells (hESCs) served as a positive control. (C) Immunofluorescence analysis demonstrated the protein expression of pluripotency markers [octamer-binding transcription factor 4 (OCT4), NANOG, TRA-1-60, and TRA-1-81] in FD-iPSCs sublines. Nuclear was counterstained with 4′,6-diamidino-2-pheylindole (DAPI). Scale bars: 200 μm. (D) In vitro three-layer differentiation of FD-iPSCs in a specific culture medium resulted in subpopulations of cells that were immunoreactive for smooth muscle actin, mesoderm (SMA), nestin, ectoderm, and α-fetoprotein, endoderm (AFP). Scale bars: 100 μm. (E) Sequence electropherograms of GLA IVS4 mutations. The nucleotide at the position 919 of IVS4 in healthy control-derived iPSCs (NC-iPSCs) or FD-iPSC sublines is indicated (arrow). The mutant allele carried guanine (G), and the wild-type allele carried alanine (A). (F) Karyotype analysis of NC- or FD-iPSCs. PBMC, peripheral blood mononuclear cell; FD1, FD-iPSC1; FD2, FD-iPSC2; SOX2, sex-determining region Y-box 2; NAT1, *N*-acetyltransferase 1; GDF3, growth differentiation factor-3; GAPDH, glyceraldehyde 3-phosphate dehydrogenase.

layer differentiation conditions, differentiated cells of both FD-iPSCs and NC-iPSCs positively stained for nestin (neuron-like cell marker for the ectoderm), SMA (smooth muscle cell marker for the mesoderm), and AFP (hepatocyte-like cell marker for the endoderm), indicating their pluripotency (Fig. 1D). The *GLA* IVS4+919G>A mutation in FD-iPSCs was confirmed through genomic DNA sequencing (Fig. 1E). The chromosomal analysis indicated that the karyotype of FD-iPSCs was identical to that of NC-iPSCs (Fig. 1F). Collectively, these results suggest that FD-iPSCs retained the genetic characteristics of the original FD clinical sample and presented the same pluripotency as that of NC-iPSCs because of the identical capabilities of cell reprogramming, stem cell gene expression, and three-germ layer differentiation.

To elucidate the mechanism underlying the pathogenesis of FD-associated vascular endothelial dysfunction, FD-iPSCs were differentiated into VECs using an established protocol[27]; a brief diagram of the protocol is presented in Figure 2A. During the differentiation procedure, the expansion and size of ECs continued to increase (Fig. 2B), indicating the induction capability of differentiating iPSCs into VECs, which has been previously described[27]. The differentiation rate of FD-iPSC-derived VECs (FD-VECs) was 13.2±2.2%, which was detected through flow cytometry against VE-cadherin, a VEC marker (Fig. 2C). After 14 days of differentiation, ECs were isolated using antibody-conjugated magnetic beads against surface CD31 (PECAM-1). The VEC characteristics of both FD-ECs and NC-ECs were similar to those of HUVECs, including the expression of the VEC markers CD31 (PECAM-1) and vWF and the capability to form vascular tube-like structures (Fig. 2D). The GLA protein level in FD-ECs was considerably lower than that in NC-ECs; however, the expression of GLA in FD-iPSCs was only slightly decreased compared with that in NC-iPSCs (Fig. 2E). These results suggest that FD-ECs expressed typical VEC characteristics and GLA reduction, representing the VEC phenotype from patients with FD. In summary, we established patient-specific FD-EC lines that carried the original genetic mutation of FD and exhibited the phenotype of GLA deficiency, providing an experimental platform for elucidating the pathophysiological mechanism of FD-associated vascular endothelial dysfunction.

Massive Lysosomal Gb3 Accumulation in FD-ECs

We observed evident accumulation of Gb3 along with the classic pathological phenotype of FD in cardiac biopsies obtained from patients with FD (Fig. 3A). Similarly, immunofluorescence staining of Gb3 demonstrated significant cellular accumulation of Gb3 in FD-ECs but not in NC-ECs (Fig. 3B). Quantification of the staining intensity indicated that, compared with NC-ECs, the accumulation of Gb3 increased by approximately 50% in FD-ECs ($p=0.009$) (Fig. 3C). Moreover, the comparative TEM analysis between FD-ECs and NC-ECs confirmed the accumulation of Gb3 in FD-ECs (Fig. 3D), and the multilayered structure was selectively observed in the lysosomes of FD-ECs, indicating lysosomal accumulation of Gb3 in FD-ECs (Fig. 3D, iii and iv). Our immunofluorescence and TEM data indicated that FD-ECs recapitulate the FD pathophysiological phenotype of intracellular lysosomal accumulation of Gb3 and can be applied in studies on FD-associated vascular endothelial dysfunction (Fig. 3E).

Increased ROS Production in FD-ECs

Abnormal accumulation of Gb3 has been associated with increased production of ROS[12]. Because of the accumulation of Gb3 in FD-ECs, we evaluated the level of intracellular ROS in iPSC-ECs through flow cytometry. As presented in Figure 4A, intracellular ROS contents, which were evaluated using DCFDA staining, were observed in FD-ECs but not in NC-ECs. The quantification of the DCFDA staining intensity through flow cytometry indicated that the production of intracellular ROS in FD-ECs was 1.6-fold higher than that in NC-ECs ($p=0.002$) (Fig. 4B). In addition, MitoSOX Red staining demonstrated significant activation of mitochondrial superoxide production in FD-ECs (Fig. 4C). The quantification of the MitoSOX Red staining intensity indicated that mitochondrial superoxide production in FD-ECs was 1.4-fold higher than that in NC-ECs ($p<0.001$) (Fig. 4D). Collectively, our results demonstrate that FD-ECs had high accumulation of Gb3 and active intracellular and mitochondrial ROS production.

Antioxidant Gene Expression Profiles in FD-ECs

Increased ROS production has been frequently correlated with impaired antioxidant gene expression. To examine the expression of antioxidant genes, we performed an RNA expression microarray analysis of hiPSCs-ECs and a comparative analysis of the expression levels of antioxidant-related genes including SODs, GPXs, glutathione S-transferase π 1 (GSTP1), glutathione S-transferase ζ 1 (GSTZ1), arachidonate 12-lipoxygenase (ALOX12), and copper chaperone for superoxide dismutase (CCS) in NC-ECs and FD-ECs. Of the selected antioxidant genes, the expression level of *SOD2* most significantly differed between FD-ECs and ND-ECs; the expression level of *SOD2* in FD-ECs was twofold lower than that in ND-ECs (Fig. 5A). The difference in the expression level of *SOD2* was further confirmed through qRT-PCR. The results revealed that compared with NC-ECs, *SOD2* mRNA levels were significantly suppressed in FD-ECs ($p=0.013$) (Fig. 5B).

To elucidate the mechanism underlying the involvement of SOD2 in vascular endothelial dysfunction, we

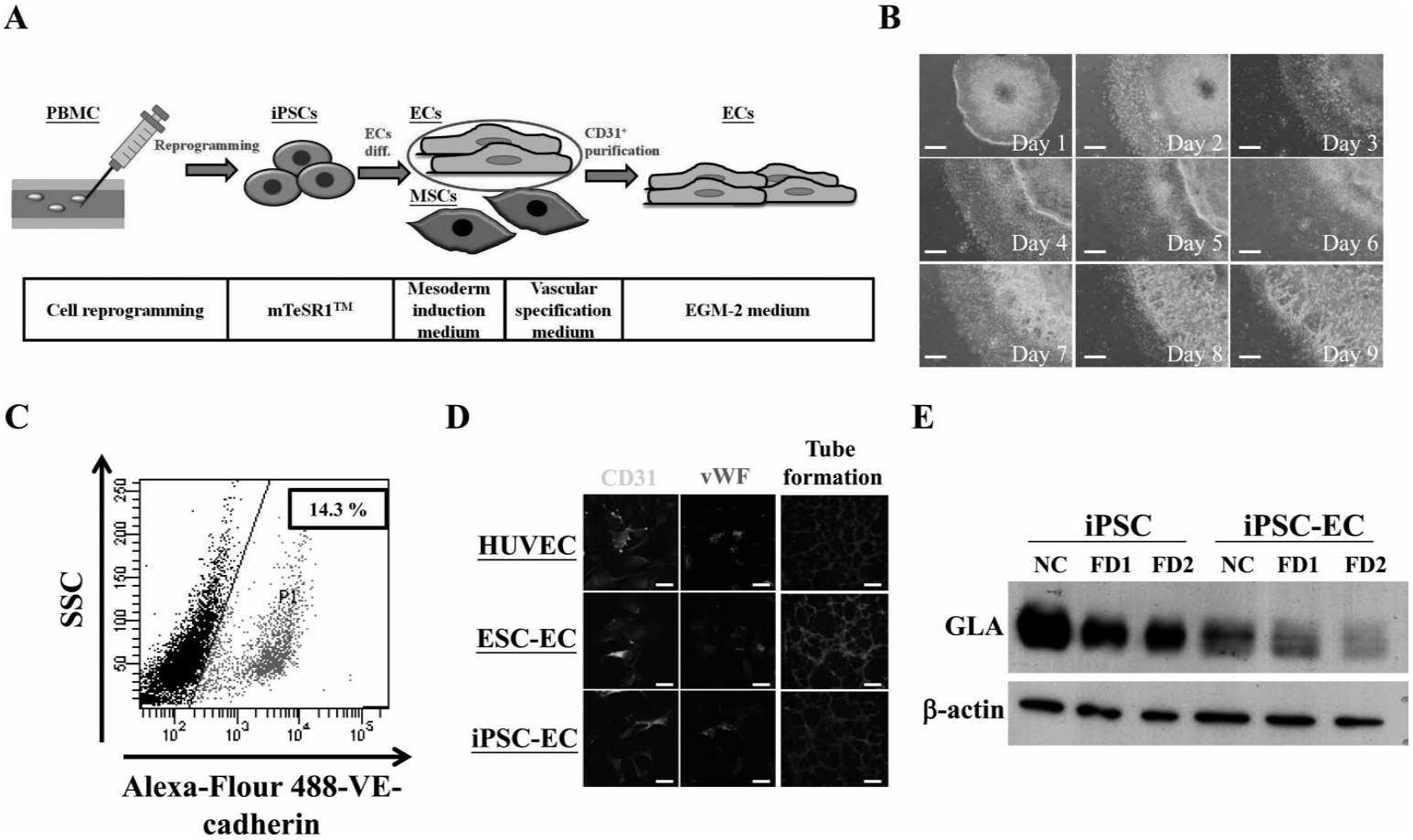

Figure 2. Characterization of Fabry disease induced pluripotent stem cell (iPSC)-derived endothelial cells (FD-ECs). (A) Schematic representation of the generation of patient-specific iPSCs and endothelial differentiation derived from iPSCs. The differentiation media are shown. (B) Morphological changes in FD-iPSCs under endothelial differentiation. Scale bars: 400 μm. (C) Represented result of rate of endothelial differentiation. Cells were stained with Alexa Fluor 488–VE-cadherin and analyzed through flow cytometry. (D) Human umbilical vein endothelial cells (HUVECs), embryonic stem cell-derived endothelial cells (ESC-ECs), or Fabry disease vascular endothelial-like cells (FD-ECs) were stained with the endothelial markers CD31 and von Willebrand factor (vWF). Scale bars: 20 μm (left and center columns). Tube formation assay was performed and stained with calcein. Scale bars: 200 μm (right column). (E) α-Galactosidase A (GLA) expression in FD-iPSCs and FD-ECs. Total cell lysates of indicated cells were collected and subjected to Western blot using GLA-specific antibodies. β-Actin served as a loading control. PBMC, peripheral blood mononuclear cell; iPSC-EC, induced pluripotent stem cell-derived endothelial cell; NC, healthy control-derived iPSCs; FD1, FD-iPSC1; FD2, FD-iPSC2.

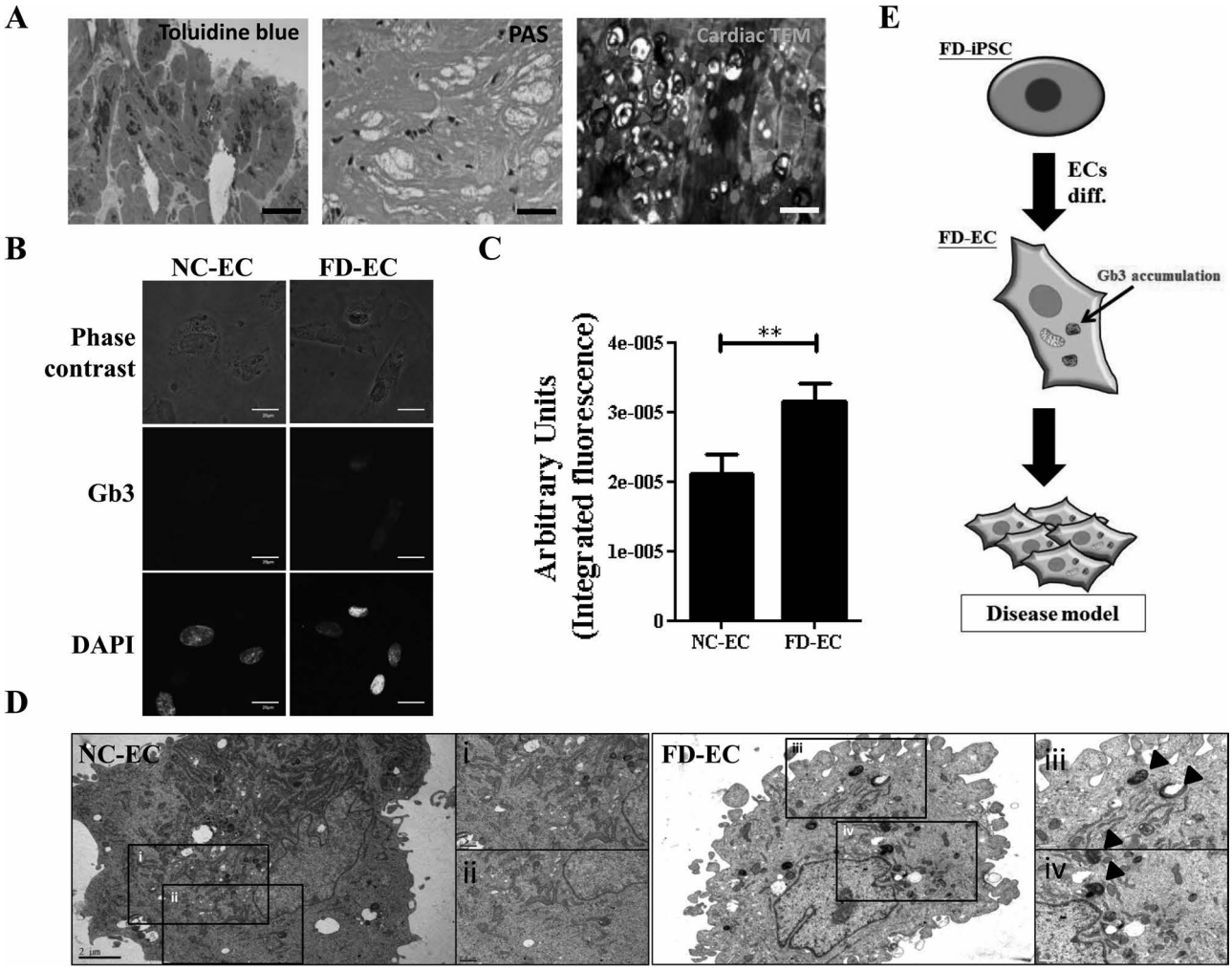

Figure 3. Gb3 accumulation in cardiac biopsy samples obtained from patients with FD and FD-iPSC-derived endothelial cells (FD-ECs). (A) Histological survey and specific staining for confirming the diagnosis of Fabry disease (FD) using cardiac biopsy samples. Toluidine blue staining of the myocardium verified the accumulation of glycosphingolipids (left). The perinuclear vacuoles were filled with materials that stained positive for periodic acid–Schiff (PAS) staining (middle). Transmission electron microscopic (TEM) examination of the myocardium revealed lamellar bodies (zebra bodies) representing lysosomes containing glycolipids, 60,000× (right). Scale bars: 250 μm. (B) Intracellular globotriaosylceramide (Gb3) in FD-ECs was stained by a Gb3-specific antibody (CD77, left). Scale bars: 20 μm. (C) The mean fluorescence intensity of an individual cell was determined using ImageJ (NIH, Bethesda, MD, USA), and quantitative data represented the fluorescence intensity of Gb3 in FD-ECs (right, $n=50$). (D) Ultrastructure of FD-ECs (10,000×). The arrowheads indicate the multilayered lysosomal structure. Scale bars: 2 μm. (E) A representative diagram of Gb3 accumulation in FD-ECs. $^{**}p<0.01$. FD-iPSC, Fabry disease induced pluripotent stem cell; DAPI, 4′,6-diamidino-2-pheylindole; NC-EC, healthy control iPSC-derived endothelial cell.

used ingenuity pathway analysis (IPA) to investigate the interaction network of SOD2 in ECs. Mapping of SOD2 to the network of "endothelial injury and abnormalities" revealed the potential factors that participate in SOD-related endothelial dysfunction. As presented in Figure 5C, SOD2 was observed to interact with the NF-κB-mediated signaling pathway that involves c-Jun N-terminal kinase (JNK), extracellular signal-regulated kinase (ERK), AKT/protein kinase B, and AMP-activated protein kinase (AMPK). Because the AMPK signaling is vital in regulating endothelial function[28], we further determined the protein expression of AMPK in FD-ECs. The phosphorylation of AMPK was significantly increased in FD-ECs accompanied with decreased SOD2 expression and GLA deficiency (Fig. 5D). A study reported that AMPK activation has a protective role in response to mitochondrial ROS production in the human endothelium[29]. In our study, AMPK activation may have further supported mitochondrial ROS production in FD-ECs. Taken together, these results suggest that SOD2, a mitochondrial

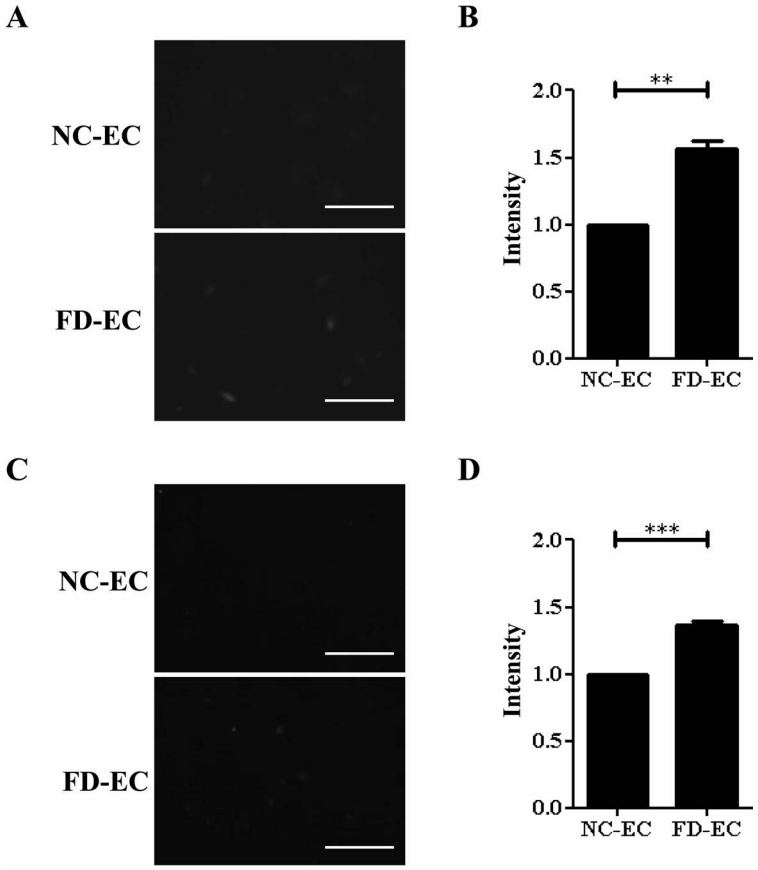

Figure 4. Accumulation of endogenous and mitochondrial ROS in FD-ECs. (A) Intracellular reactive oxygen species (ROS) in Fabry disease (FD) induced pluripotent stem cell-derived vascular endothelial-like cells (FD-ECs) was stained using 2′,7′-dichlorofluorescin diacetate (DCFDA), and (B) fluorescence intensity was measured through flow cytometry. The expression level of healthy control iPSC-derived endothelial cells (NC-ECs) served as 1. Data are presented as mean ± standard error of the mean (SEM), $n = 4$. Scale bars: 200 μm. (C) Mitochondrial ROS in FD-ECs was stained using MitoSOX Red, and (D) fluorescence intensity was measured through flow cytometry. NC-ECs served as 1. Data are presented as mean ± SEM, $n = 4$. $^{**}p < 0.01$; $^{***}p < 0.001$. Scale bars: 200 μm.

antioxidant enzyme, plays a crucial role, at least in part, in increasing ROS contents in FD-ECs.

Gb3 Administration, But Not GLA Deficiency, Reduced SOD2 Expression in VECs

The low expression of SOD2 in FD-ECs might be attributable to the loss of GLA expression or cellular accumulation of Gb3. To confirm this notion, we knocked down GLA expression using shRNAs in HUVECs and evaluated changes in SOD2 mRNA and protein levels. The results of qRT-PCR and Western blot revealed that GLA shRNA successfully reduced GLA expression; however, unlike what we expected, mRNA or protein levels of SOD2 were not suppressed after the knockdown of GLA (Fig. 6A and B). These results ruled out the possibility that GLA deficiency suppresses SOD2 expression in FD-ECs. To determine the effect of Gb3 accumulation on SOD2 expression, a Gb3–BSA conjugant was administered to HUVECs. The protein expression level of SOD2 in HUVECs significantly decreased after Gb3 treatment in a dose-dependent manner ($p = 0.036$) (Fig. 7A and B). In addition, AMPK activation significantly increased in HUVECs after treatment with 100 μM Gb3 ($p = 0.039$) (Fig. 7A and C). Furthermore, qRT-PCR results confirmed that Gb3 administration selectively decreased SOD2 mRNA expression ($p = 0.002$) (Fig. 7D), which is in line with the phenomenon of FD-ECs (Fig. 5B and D). To confirm that GLA plays a vital role in Gb3-mediated SOD2 downregulation, HUVECs were simultaneously treated with rhα-GLA and Gb3. We observed that rhα-GLA significantly rescued Gb3-induced SOD2 reduction in HUVECs (Fig. 7E). Collectively, our results indicate that Gb3 accumulation reduces SOD2 expression in FD-ECs, which may consequently increase ROS production. Furthermore, we determined that SOD2 expression decreased due to Gb3 accumulation and not due to GLA deficiency in HUVECs, suggesting a detrimental role of Gb3 accumulation in redox homeostasis of FD-ECs and a

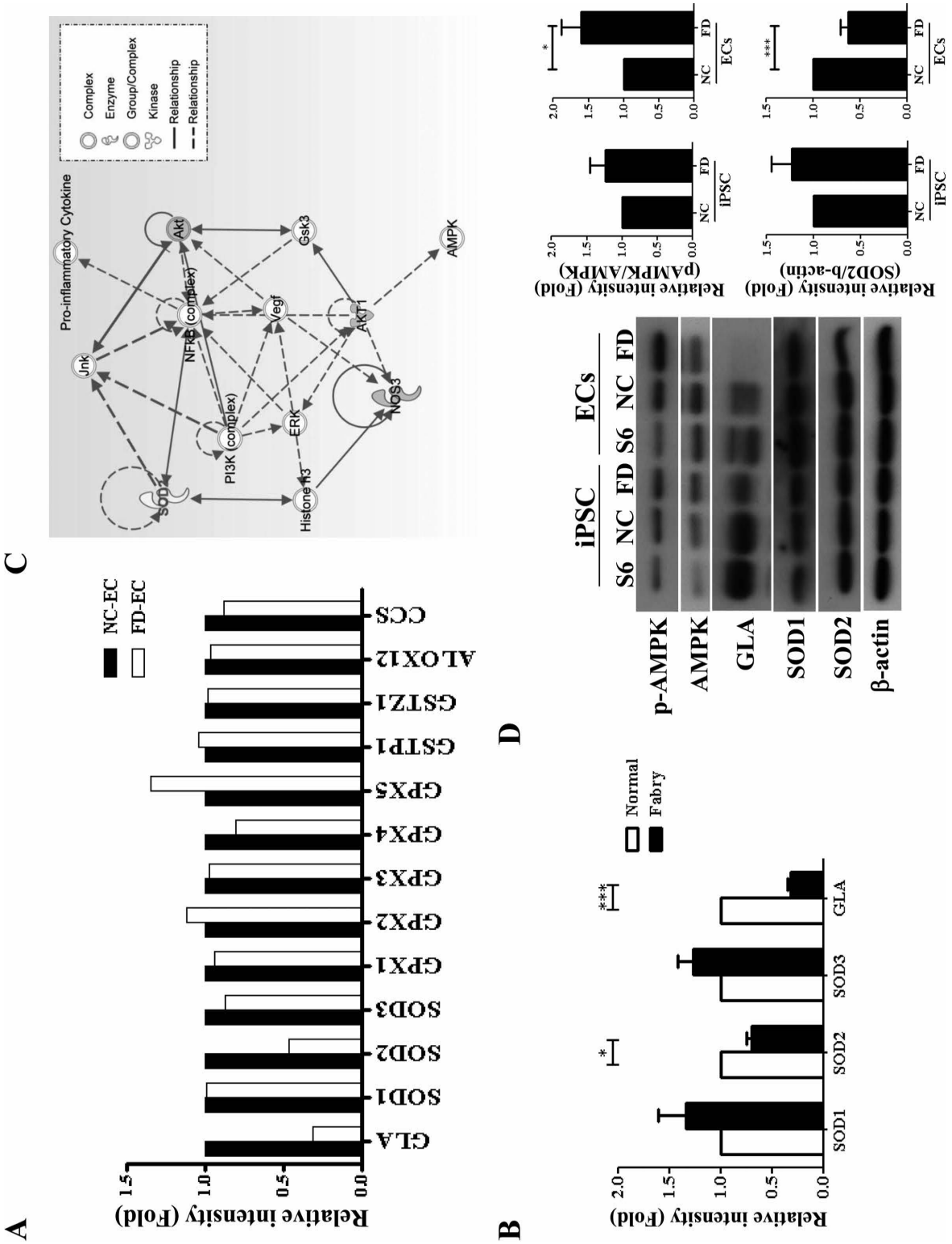

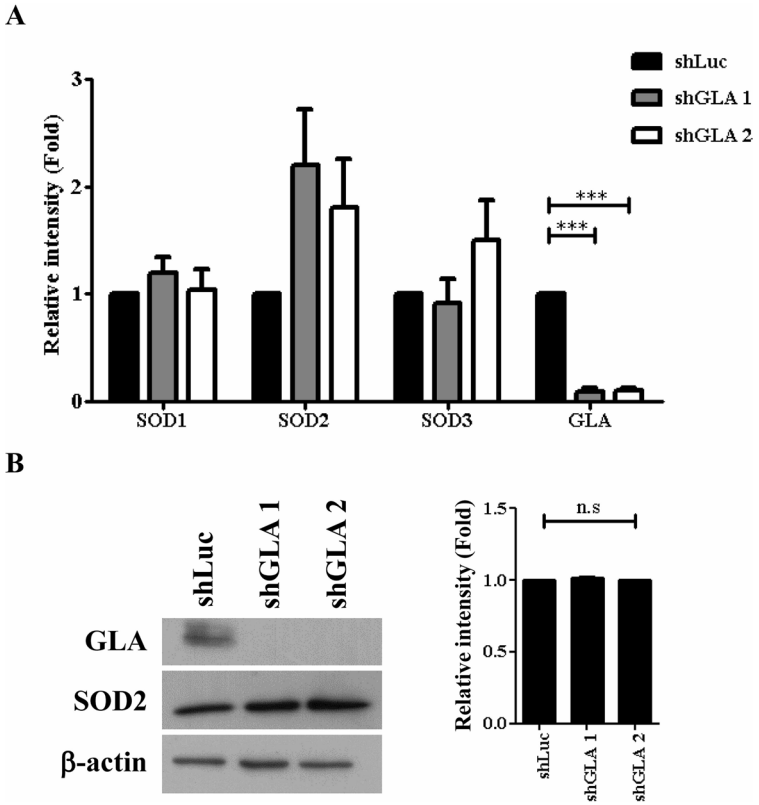

Figure 6. Detection of SOD2 expression in HUVECs treated with GLA shRNA. (A) α-Galactosidase A (GLA) silencing after transfection of human umbilical vein endothelial cells (HUVECs) with GLA shRNA. Total RNA from HUVECs transfected with the indicated shRNA was collected and subjected to quantitative real-time polymerase chain reaction (qRT-PCR) analysis. Values were representative of four independent experiments; all blots were normalized to the glyceraldehyde 3-phosphate dehydrogenase (GAPDH) expression. Small hairpin RNA specific for luciferase (shLuc) served as 1. (B) Protein expression of GLA and superoxide dismutase 2 (SOD2) in GLA shRNA-treated HUVECs. Total cell lysates of indicated cells were collected and subjected to Western blot by using GLA- or SOD2-specific antibodies, respectively. β-Actin served as a loading control (left). Quantitative data are presented as mean±standard error of the mean (SEM) of three independent experiments (right). ***$p<0.001$ compared to cells transfected with small hairpin RNA specific for luciferase (shLuc).

FACING PAGE

Figure 5. Dysregulated expression levels of the antioxidant enzyme in FD-ECs. (A) Data of antioxidant-related gene expressions from microarray analysis. (B) Expression of superoxide dismutases (SODs). Total RNA from indicated cells was collected and subjected to quantitative real-time polymerase chain reaction (qRT-PCR) analysis using specific primer sets; all blots were normalized to the glyceraldehyde 3-phosphate dehydrogenase (GAPDH) expression. The expression level of healthy control induced pluripotent stem cell-derived endothelial cells (NC-ECs) served as 1. Data are presented as mean±standard error of the mean (SEM), $n=4$. (C) The associated network was defined using ingenuity pathway analysis (IPA) for SOD2 and endothelial dysfunction-related genes. (D) Protein expression of ROS-related proteins in Fabry disease induced pluripotent stem cells (FD-iPSCs) and Fabry disease (FD) induced pluripotent stem cell-derived vascular endothelial-like cells (FD-ECs). Total cell lysates of indicated cells were collected and subjected to Western blot using phospho-AMP-activated protein kinase (p-AMPK)-, AMPK-, α-galactosidase A (GLA)-, SOD1-, or SOD2-specific antibodies, respectively. β-Actin served as a loading control. Quantitative data are presented as mean±SEM of three independent experiments. *$p<0.05$; ***$p<0.001$. GPXs, catalase and glutathione peroxidases; GSTP1, glutathione S-transferase π 1; GSTZ1, glutathione S-transferase ζ 1; ALOX12, arachidonate 12-lipoxygenase; CCS, copper chaperone for superoxide dismutase; S6, human embryonic stem cell; GSK3, glycogen synthase kinase 3; NF-κB, nuclear transcription factor κB; PI3K, phosphatidylinositol-3-kinase; NOS3, nitric oxide synthase 3; VEGF, vascular endothelial growth factor; JNK, Jun N-terminal kinase; ERK, extracellular signal-regulated kinase.

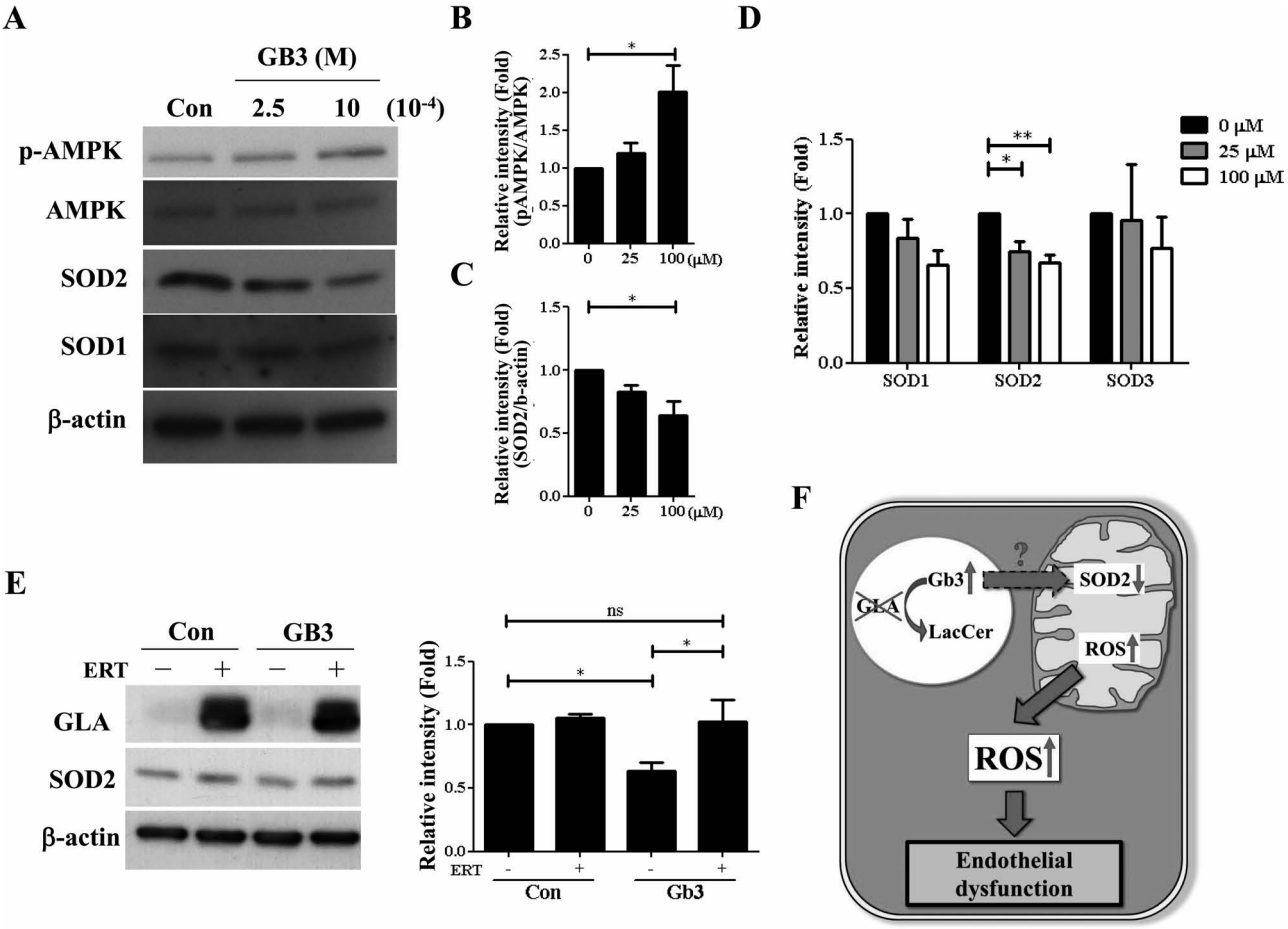

Figure 7. Ectopic addition of Gb3 suppressed SOD2 expression in HUVECs. (A) Globotriaosylceramide (Gb3) suppressed superoxide dismutase 2 (SOD2) expression in human umbilical vein endothelial cells (HUVECs). HUVECs were incubated with the indicated concentration of Gb3 for 48 h. After several washes, lysates were subjected to Western blot using phospho-AMP-activated protein kinase (p-AMPK)-, AMPK-, SOD1-, or SOD2-specific antibodies, respectively. β-Actin served as a loading control. (B, C) Quantitative data of (A) presented the mean ± standard error of the mean (SEM) of three independent experiments. (D) Total RNA from HUVECs treated with the indicated concentration of Gb3 was subjected to quantitative real-time polymerase chain reaction (qRT-PCR) analysis. The RNA expression of indicated antioxidant proteins was quantified using specific primer sets; all blots were normalized to the glyceraldehyde 3-phosphate dehydrogenase (GAPDH) expression. The untreated group served as 1. Data are presented as mean ± SEM, $n = 4$. (E) HUVECs were incubated with recombinant human α-galactosidase (rhα-GLA) (5 μg/ml) or Gb3 (100 μM) for 48 h. After several washes, the lysates were subjected to Western blot analysis using GLA- or SOD2-specific antibodies, respectively. β-Actin served as a loading control. Quantitative data are presented as mean ± SEM, $n = 4$. (F) Schematic representation of GLA deficiency-induced cellular reactive oxygen species (ROS) production. *$p < 0.05$; **$p < 0.01$. LacCer, lactosylceramide; Con, control.

consequent effect on FD-associated vascular endothelial dysfunction (Fig. 7F).

DISCUSSION

The progressive accumulation of Gb3 has been considered to play a critical pathophysiological role in FD-associated cardiovascular disorders[1,2,30]. In addition, clinical studies have reported higher oxidative stress and oxidative stress-induced damage from protein to DNA[13,31]. Oxidative stress plays a crucial role in the development of atherosclerosis and other cardiovascular disorders through the oxidation of low-density lipoproteins and modification of endothelial functions and adhesion molecules[32,33]. A clinical study reported that VEGF-A, an oxidative stress-induced factor, was increased in a patient with FD and that a high VEGF-A level is a possible response to vascular damage[34]. These studies have suggested the potential involvement of oxidative stress in the pathogenesis of vascular complications in FD. However, detailed mechanisms underlying the effect of Gb3 on the deregulation of pathological factors remain largely unclear. In this study, we determined that Gb3 accumulation is

accompanied with an increase in ROS production, supporting the effect of Gb3 on oxidative stress in VECs.

We performed a microarray analysis to identify the critical role of SOD2 in Gb3-induced oxidative stress in VECs. The causality of Gb3 in the suppression of SOD2 expression has been determined in HUVECs. SOD2 is located in the mitochondrial matrix and can scavenge the superoxide leaking from the respiratory chain[19]. The suppression of SOD2 production by siRNA resulted in the overproduction of ROS, loss of mitochondrial membrane potential, and induction of the apoptotic program in rabbit corneal ECs[23]. Furthermore, homozygous (*Sod2*$^{-/-}$) knockout was lethal in neonatal mice and resulted in dilated cardiomyopathy and severe myocardial tissue damage[35,36]. In addition, mice with *Sod2* heterozygous mutation (*Sod2*$^{+/-}$) exhibit endothelial dysfunction with hypercholesterolemia[20] and aging[21]. Moreover, a study reported decreased SOD2 expression in the circulating angiogenic cells of a patient with FD[37]. Mitochondrial haplogroup variants account for different mitochondrial functions such as ATP production, ROS generation, and calcium buffering. Specific mitochondrial haplogroups are more frequently observed in patients with FD, indicating a role of mitochondria in FD[38]. Taken together, our results indicate that Gb3-induced increased ROS production and mitochondrial SOD2 suppression may play a role, at least in part, in FD-associated vascular endothelial dysfunction.

NF-κB has been regarded as a redox-sensitive transcription factor that manipulates homeostasis and endothelial inflammatory responses[39]. JNK, a stress-activated protein kinase, participates in ROS-induced endothelial dysfunction[40]. In addition, the involvement of several downstream effectors of JNK and/or NF-κB signaling [i.e., ERK, phosphoinositide 3-kinase (PI3K), AKT/protein kinase B, nitric oxide synthase 3 (NOS3), and AMPK] has been demonstrated by IPA. All these signaling molecules play crucial roles in the maintenance of physiological homeostasis in VECs[39,41,42]. The activation of AMPK plays a vital role in the modulation of endothelial functions under stress[28,43]. A recent study reported that increased mitochondrial ROS production significantly enhanced AMPK activation in the endothelium of patients with coronary artery disease and type 2 diabetes[29]. The protective role of AMPK activation in response to oxidative stress[44,45] further supports our findings that Gb3 suppressed SOD2 expression causing an increase in ROS production along with enhancing AMPK activation (p-AMPK). However, prolonged AMPK activation causes vascular endothelial impairment[46], suggesting that Gb3-induced AMPK activation has an etiological role in FD-associated vascular dysfunction. Therefore, more studies are required to investigate whether the interplay between AMPK and mitochondrial SOD2 regulates the imbalance of FD-associated oxidative stress in patients with FD and cardiovascular diseases. Overall, our bioinformatics approach of gene regulatory linkage analysis indicated that SOD2 is a major constituent in the network of FD-associated oxidative stress, strengthening the involvement of mitochondrial SOD2 in FD-associated vascular endothelial dysfunction.

The GLA protein expression level was considerably lower in FD-ECs than in NC-ECs, and this phenomenon correlates with the severe pathophysiological phenotype of FD-ECs. A study reported a high incidence of the *GLA* IVS4+919G>A mutation (approximately 1 in 1,500–1,600 men) in patients with FD having the late-onset cardiac phenotype in Taiwan[5,47]. Therefore, this finding provides a possible mechanism for the late-onset cardiac phenotype in which the *GLA* IVS4+919G>A mutation is expressed. This notion should be explored in future studies using the IVS4+919G>A mutation and hiPSCs derived from patients with classical FD. In conclusion, our study findings were as follows: (1) VECs carrying the *GLA* IVS4+919G>A mutation had increased ROS production and Gb3 accumulation; (2) FD-ECs exhibited decreased expression of the antioxidant SOD2 and accumulation of Gb3; and (3) administration of Gb3, but not knockdown of GLA, in part, suppressed mitochondrial SOD2 expression in VECs. The imbalance of the redox status leads to endothelial dysfunction through canonical cell death and inflammation. The newly defined interplay among GLA, Gb3, and SOD2 reveals a potential pathophysiological mechanism that causes increased ROS production and provides insights on targets that can be used for developing novel therapeutics for FD, particularly for severe FD-associated cardiovascular complications.

ACKNOWLEDGMENTS: The authors thank Dr. De-Kuang Hwang for his assistance in statistical analyses. This study was funded by the MOST and National Science Council (103-2321-B-010-025, 104-2627-M-010-004, 104-2325-B-010-006, 105-2633-B-009-003, and 105-3011-B010-001), Academia Sinica and MOST (MOST 104-0210-01-09-02 and 105-0210-01-13-01), Taipei Veterans General Hospital (Stem Cell Project E99-105), Taipei Veterans General Hospital intramural grant (V103C-166, V104C-175, V104D14-003-MY3-2, V104E14-001-MY3-3, V105C-189, and V105C-077), Research Foundation of Cardiovascular Medicine, the Department of Health Cancer Center Research of Excellence (MOHW104-TDU-B-211-124-001/TD-B-111-02, MOHW104-TDU-B-211-113-003, MOHW105-TDU-B-211-134003, and MOHW105-TDU-B-211-133017), Yen-Tjing-Ling Medical Foundation (CI-102-105), National Health Research Institutes (NHRI-EX102-10258SI), NRPB Human iPSC Alliance-Core Service (MOST104-2325-B-001-010 and MOST 105-2325-B-010-005), VGH, TSGH, NDMC, AS Joint Research Program (VTA105-V1-5-1), TVGH-NTU Joint Project (VN104-09), and the Genomic Center Project and Cancer Center Project of National Yang-Ming University (Ministry of Education, Aim for the Top University Plan), Taiwan. We thank Miss Su-Hua Chiang, Chia-Ling Wang, Yi-Ching Tsai, and Dr. Hsian-Guey Hsieh for their help in the hiPSC technique. The authors declare no conflicts of interest.

REFERENCES

1. Desnick RJ, Wasserstein MP, Banikazemi M. Fabry disease (alpha-galactosidase A deficiency): Renal involvement and enzyme replacement therapy. Contrib Nephrol. 2001(136):174–92.
2. Zarate YA, Hopkin RJ. Fabry's disease. Lancet 2008; 372(9647):1427–35.
3. Human Gene Mutation Database. QIAGEN: Cardiff University. Available from http://www.hgmd.cf.ac.uk/ac/index.php
4. Lin HY, Chong KW, Hsu JH, Yu HC, Shih CC, Huang CH, Lin SJ, Chen CH, Chiang CC, Ho HJ, Lee PC, Kao CH, Cheng KH, Hsueh C, Niu DM. High incidence of the cardiac variant of Fabry disease revealed by newborn screening in the Taiwan Chinese population. Circ Cardiovasc Genet. 2009;2(5):450–6.
5. Hwu WL, Chien YH, Lee NC, Chiang SC, Dobrovolny R, Huang AC, Yeh HY, Chao MC, Lin SJ, Kitagawa T, Desnick RJ, Hsu LW. Newborn screening for Fabry disease in Taiwan reveals a high incidence of the later-onset GLA mutation c.936+919G>A (IVS4+919G>A). Hum Mutat. 2009;30(10):1397–405.
6. Chien YH, Lee NC, Chiang SC, Desnick RJ, Hwu WL. Fabry disease: Incidence of the common later-onset alpha-galactosidase A IVS4+919G→A mutation in Taiwanese newborns—Superiority of DNA-based to enzyme-based newborn screening for common mutations. Mol Med. 2012; 18:780–4.
7. Mitsias P, Levine SR. Cerebrovascular complications of Fabry's disease. Ann Neurol. 1996;40(1):8–17.
8. Boutouyrie P, Laurent S, Laloux B, Lidove O, Grunfeld JP, Germain DP. Non-invasive evaluation of arterial involvement in patients affected with Fabry disease. J Med Genet. 2001;38(9):629–31.
9. Altarescu G, Moore DF, Pursley R, Campia U, Goldstein S, Bryant M, Panza JA, Schiffmann R. Enhanced endothelium-dependent vasodilation in Fabry disease. Stroke 2001;32 (7):1559–62.
10. Namdar M, Gebhard C, Studiger R, Shi Y, Mocharla P, Schmied C, Brugada P, Luscher TF, Camici GG. Globotriaosylsphingosine accumulation and not alpha-galactosidase—A deficiency causes endothelial dysfunction in Fabry disease. PLoS One 2012;7(4):e36373.
11. Choi S, Kim JA, Na HY, Cho SE, Park S, Jung SC, Suh SH. Globotriaosylceramide induces lysosomal degradation of endothelial KCa3.1 in Fabry disease. Arterioscler Thromb Vasc Biol. 2014;34(1):81–9.
12. Shen JS, Meng XL, Moore DF, Quirk JM, Shayman JA, Schiffmann R, Kaneski CR. Globotriaosylceramide induces oxidative stress and up-regulates cell adhesion molecule expression in Fabry disease endothelial cells. Mol Genet Metab. 2008;95(3):163–8.
13. Biancini GB, Vanzin CS, Rodrigues DB, Deon M, Ribas GS, Barschak AG, Manfredini V, Netto CB, Jardim LB, Giugliani R, Vargas CR. Globotriaosylceramide is correlated with oxidative stress and inflammation in Fabry patients treated with enzyme replacement therapy. Biochim Biophys Acta 2012;1822(2):226–32.
14. Alexander RW. Theodore Cooper Memorial Lecture. Hypertension and the pathogenesis of atherosclerosis. Oxidative stress and the mediation of arterial inflammatory response: A new perspective. Hypertension 1995;25(2): 155–61.
15. Ross R. Atherosclerosis is an inflammatory disease. Am Heart J. 1999;138(5 Pt 2):S419–20.
16. Satoh K, Shimokawa H, Berk BC. Cyclophilin A: Promising new target in cardiovascular therapy. Circ J. 2010;74(11):2249–56.
17. Levonen AL, Vahakangas E, Koponen JK, Yla-Herttuala S. Antioxidant gene therapy for cardiovascular disease: Current status and future perspectives. Circulation 2008; 117(16):2142–50.
18. Li Y, Huang TT, Carlson EJ, Melov S, Ursell PC, Olson JL, Noble LJ, Yoshimura MP, Berger C, Chan PH, Wallace DC, Epstein CJ. Dilated cardiomyopathy and neonatal lethality in mutant mice lacking manganese superoxide dismutase. Nat Genet. 1995;11(4):376–81.
19. Murphy MP. How mitochondria produce reactive oxygen species. Biochem J. 2009;417(1):1–13.
20. Ohashi M, Runge MS, Faraci FM, Heistad DD. MnSOD deficiency increases endothelial dysfunction in ApoE-deficient mice. Arterioscler Thromb Vasc Biol. 2006;26(10): 2331–6.
21. Brown KA, Didion SP, Andresen JJ, Faraci FM. Effect of aging, MnSOD deficiency, and genetic background on endothelial function: Evidence for MnSOD haploinsufficiency. Arterioscler Thromb Vasc Biol. 2007;27(9):1941–6.
22. Ballinger SW, Patterson C, Knight-Lozano CA, Burow DL, Conklin CA, Hu Z, Reuf J, Horaist C, Lebovitz R, Hunter GC, McIntyre K, Runge MS. Mitochondrial integrity and function in atherogenesis. Circulation 2002;106(5):544–9.
23. Liu C, Ogando D, Bonanno JA. SOD2 contributes to antioxidative capacity in rabbit corneal endothelial cells. Mol Vis. 2011;17:2473–81.
24. Park IH, Arora N, Huo H, Maherali N, Ahfeldt T, Shimamura A, Lensch MW, Cowan C, Hochedlinger K, Daley GQ. Disease-specific induced pluripotent stem cells. Cell 2008;134(5):877–86.
25. Itier JM, Ret G, Viale S, Sweet L, Bangari D, Caron A, Le-Gall F, Benichou B, Leonard J, Deleuze JF, Orsini C. Effective clearance of GL-3 in a human iPSC-derived cardiomyocyte model of Fabry disease. J Inherit Metab Dis. 2014;37(6):1013–22.
26. Chang YC, Chang WC, Hung KH, Yang DM, Cheng YH, Liao YW, Woung LC, Tsai CY, Hsu CC, Lin TC, Liu JH, Chiou SH, Peng CH, Chen SJ. The generation of induced pluripotent stem cells for macular degeneration as a drug screening platform: Identification of curcumin as a protective agent for retinal pigment epithelial cells against oxidative stress. Front Aging Neurosci. 2014;6:191.
27. Orlova VV, van den Hil FE, Petrus-Reurer S, Drabsch Y, Ten Dijke P, Mummery CL. Generation, expansion and functional analysis of endothelial cells and pericytes derived from human pluripotent stem cells. Nat Protoc. 2014;9(6):1514–31.
28. Fisslthaler B, Fleming I. Activation and signaling by the AMP-activated protein kinase in endothelial cells. Circ Res. 2009;105(2):114–27.
29. Mackenzie RM, Salt IP, Miller WH, Logan A, Ibrahim HA, Degasperi A, Dymott JA, Hamilton CA, Murphy MP, Delles C, Dominiczak AF. Mitochondrial reactive oxygen species enhance AMP-activated protein kinase activation in the endothelium of patients with coronary artery disease and diabetes. Clin Sci (Lond) 2013;124(6):403–11.
30. Eng CM, Guffon N, Wilcox WR, Germain DP, Lee P, Waldek S, Caplan L, Linthorst GE, Desnick RJ. Safety and efficacy of recombinant human alpha-galactosidase A—Replacement therapy in Fabry's disease. N Engl J Med. 2001;345(1):9–16.

31. Biancini GB, Moura DJ, Manini PR, Faverzani JL, Netto CB, Deon M, Giugliani R, Saffi J, Vargas CR. DNA damage in Fabry patients: An investigation of oxidative damage and repair. Mutat Res Genet Toxicol Environ Mutagen 2015;784–785:31–6.
32. Madamanchi NR, Vendrov A, Runge MS. Oxidative stress and vascular disease. Arterioscler Thromb Vasc Biol. 2005; 25(1):29–38.
33. Stocker R, Keaney JF Jr. Role of oxidative modifications in atherosclerosis. Physiol Rev. 2004;84(4):1381–478.
34. Zampetti A, Gnarra M, Borsini W, Giurdanella F, Antuzzi D, Piras A, Smaldone C, Pieroni M, Cadeddu C, de Waure C, Feliciani C. Vascular endothelial growth factor (VEGF-a) in Fabry disease: Association with cutaneous and systemic manifestations with vascular involvement. Cytokine 2013;61(3):933–9.
35. Huang TT, Carlson EJ, Gillespie AM, Epstein CJ. Genetic modification of the dilated cardiomyopathy and neonatal lethality phenotype of mice lacking manganese superoxide dismutase. Age (Omaha) 1998;21(2):83–4.
36. Lebovitz RM, Zhang H, Vogel H, Cartwright J, Jr., Dionne L, Lu N, Huang S, Matzuk MM. Neurodegeneration, myocardial injury, and perinatal death in mitochondrial superoxide dismutase-deficient mice. Proc Natl Acad Sci USA 1996;93(18):9782–7.
37. Lorenzen JM, Dietrich B, Fiedler J, Jazbutyte V, Fleissner F, Karpinski N, Weidemann F, Wanner C, Asan E, Caprio M, Ertl G, Bauersachs J, Thum T. Pathologic endothelial response and impaired function of circulating angiogenic cells in patients with Fabry disease. Basic Res Cardiol. 2013;108(1):311.
38. Simoncini C, Chico L, Concolino D, Sestito S, Fancellu L, Boadu W, Sechi GP, Feliciani C, Gnarra M, Zampetti A, Salviati A, Scarpelli M, Orsucci D, Bonuccelli U, Siciliano G, Mancuso M. Mitochondrial DNA haplogroups may influence Fabry disease phenotype. Neurosci Lett. 2016;629:58–61.
39. Sena CM, Pereira AM, Seica R. Endothelial dysfunction—A major mediator of diabetic vascular disease. Biochim Biophys Acta 2013;1832(12):2216–31.
40. Fu YC, Yin SC, Chi CS, Hwang B, Hsu SL. Norepinephrine induces apoptosis in neonatal rat endothelial cells via a ROS-dependent JNK activation pathway. Apoptosis 2006; 11(11):2053–63.
41. Rajendran P, Rengarajan T, Thangavel J, Nishigaki Y, Sakthisekaran D, Sethi G, Nishigaki I. The vascular endothelium and human diseases. Int J Biol Sci. 2013;9(10):1057–69.
42. De Nigris F, Lerman LO, Condorelli M, Lerman A, Napoli C. Oxidation-sensitive transcription factors and molecular mechanisms in the arterial wall. Antioxid Redox Signal. 2001;3(6):1119–30.
43. Nagata D, Mogi M, Walsh K. AMP-activated protein kinase (AMPK) signaling in endothelial cells is essential for angiogenesis in response to hypoxic stress. J Biol Chem. 2003;278(33):31000–6.
44. Wu SB, Wu YT, Wu TP, Wei YH. Role of AMPK-mediated adaptive responses in human cells with mitochondrial dysfunction to oxidative stress. Biochim Biophys Acta 2014;1840(4):1331–44.
45. Shafique E, Choy WC, Liu Y, Feng J, Cordeiro B, Lyra A, Arafah M, Yassin-Kassab A, Zanetti AV, Clements RT, Bianchi C, Benjamin LE, Sellke FW, Abid MR. Oxidative stress improves coronary endothelial function through activation of the pro-survival kinase AMPK. Aging (Albany NY) 2013;5(7):515–30.
46. Turkseven S, Ertuna E. Prolonged AMP-activated protein kinase induction impairs vascular functions. Can J Physiol Pharmacol. 2013;91(12):1025–30.
47. Ishii S, Nakao S, Minamikawa-Tachino R, Desnick RJ, Fan JQ. Alternative splicing in the alpha-galactosidase A gene: Increased exon inclusion results in the Fabry cardiac phenotype. Am J Hum Genet. 2002;70(4):994–1002.